Title
Internal Structure and Preferential Protein Binding of Colloidal Aggregates

Journal
ACS Chemical Biology, 12(1)

ISSN
1554-8929

Authors
Duan, Da
Torosyan, Hayarpi
Elnatan, Daniel
et al.

Publication Date
2017-01-20

DOI
10.1021/acschembio.6b00791

Peer reviewed

HHS Public Access

Author manuscript

ACS Chem Biol. Author manuscript; available in PMC 2018 January 20.

Published in final edited form as:

ACS Chem Biol. 2017 January 20; 12(1): 282–290. doi:10.1021/acschembio.6b00791.

Internal Structure and Preferential Protein Binding of Colloidal Aggregates

Da Duan[†,⊥], **Hayarpi Torosyan**[†,⊥], **Daniel Elnatan**[‡,⊥], **Christopher K. McLaughlin**[§,‖], **Jennifer Logie**[§,‖], **Molly S. Shoichet**[§,‖], **David A. Agard**[*,‡], and **Brian K. Shoichet**[*,†]

[†]Department of Pharmaceutical Chemistry & Quantitative Biology Institute, University of California, San Francisco, 1700 Fourth Street, San Francisco, California 94158-2550, United States

[‡]Howard Hughes Medical Institute and the Department of Biochemistry and Biophysics, University of California, San Francisco, San Francisco, California 94158, United States

[§]Department of Chemical Engineering and Applied Chemistry, University of Toronto, 200 College Street, Toronto, Ontario, Canada M5S 3E5

[‖]Institute of Biomaterials and Biomedical Engineering, University of Toronto, 164 College Street, Toronto, Ontario, Canada M5S 3G9

Abstract

Colloidal aggregates of small molecules are the most common artifact in early drug discovery, sequestering and inhibiting target proteins without specificity. Understanding their structure and mechanism has been crucial to developing tools to control for, and occasionally even exploit, these particles. Unfortunately, their polydispersity and transient stability have prevented exploration of certain elementary properties, such as how they pack. Dye-stabilized colloidal aggregates exhibit enhanced homogeneity and stability when compared to conventional colloidal aggregates, enabling investigation of some of these properties. By small-angle X-ray scattering and multiangle light scattering, pair distance distribution functions suggest that the dye-stabilized colloids are filled, not hollow, spheres. Stability of the coformulated colloids enabled investigation of their preference for binding DNA, peptides, or folded proteins, and their ability to purify one from the other. The coformulated colloids showed little ability to bind DNA. Correspondingly, the colloids preferentially sequestered protein from even a 1600-fold excess of peptides that are themselves the result of a digest of the same protein. This may reflect the avidity advantage that a protein has in a surface-to-surface interaction with the colloids. For the first time, colloids could be shown to have preferences of up to 90-fold for particular proteins over others. Loaded onto the colloids, bound

[*]**Corresponding Authors:** agard@msg.ucsf.edu; bshoichet@gmail.com.
[⊥]Contributed equally.

Supporting Information

The Supporting Information is available free of charge on the ACS Publications website at DOI: 10.1021/acschem-bio.6b00791.
Supporting Figure 1 (PDF)

ORCID

Molly S. Shoichet: 0000-0003-1830-3475
Brian K. Shoichet: 0000-0002-6098-7367

Notes

The authors declare no competing financial interest.

enzyme could be spun down, resuspended, and released back into buffer, regaining most of its activity. Implications of these observations for colloid mechanisms and utility will be considered.

Graphical abstract

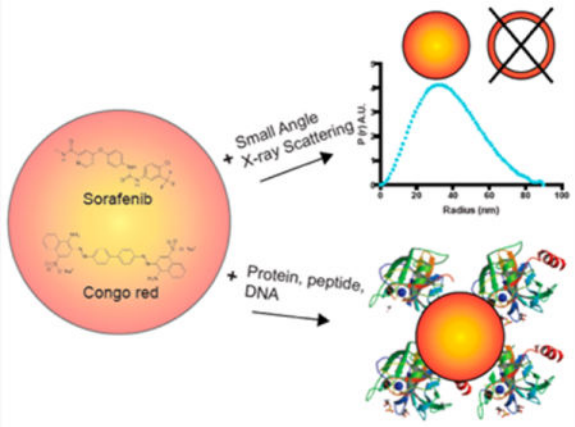

At micromolar and submicromolar concentrations, many drugs, reagents, and hits from high-throughput screening (HTS) aggregate to form colloids in aqueous buffer.[1,2] Once formed, these colloids bind and nonspecifically inhibit (and occasionally activate[3]) most proteins.[4,5] This promiscuous activity is the dominant artifact in early ligand discovery,[6–13] with 85 to 95% of hits attributable to this effect in assays that do not control for it (PAINS mechanisms,[14–16] always present, emerge prominently in assays that do control for aggregation). Accordingly, much effort has been devoted to characterizing the occurrence and mechanism of colloidal aggregators.[6,17–20] Colloid formation occurs *via* a phase-like transition that passes through a critical aggregation concentration (CAC),[2,21,22] akin to a critical micelle concentration (CMC), where liquid colloids rapidly appear.[23] Once formed, the colloids physically sequester proteins,[4] binding them with subnanomolar K_d values[2,24] and partially denaturing them.[25] Key aspects of their structure and mechanism have remained elusive, however, owing to their physical properties and instability. For instance, whereas comparison of colloid to monomer volumes has suggested that colloids might be well-packed,[2] polydispersity and transient stability have made investigating this difficult.

Recently, coformulation of colloids with azo-dyes has improved their homogeneity.[26] These coformulations consist of well-known aggregators such as sorafenib or vemurafenib mixed with small molar ratios of dyes such as Congo Red or Evans Blue. For example, a molar ratio of 25:1 of sorafenib to Congo red results in colloids of radii ~33 nm that are far more homogeneous in size than pure compound colloids. These newly formulated colloids may be maintained suspended in buffer for over 3 days without detectable precipitation[26] and then may be disrupted to release bound protein cargo that has suffered little loss of activity. Indeed, enzymes bound to the colloids retained much more activity than those free in solution, suggesting that the colloids acted almost as chaperones.[26]

Here, we exploit the homogeneity of these previously characterized colloidal coformulations,[26] treating them as model systems that allow us to investigate colloid internal

structure. This we do by small-angle X-ray scattering (SAXS), dynamic light scattering (DLS), and multiangle light scattering (MALS), initially asking simply whether these colloidal aggregates are well-packed or hollow? This fundamental question could not be previously answered because the heterogeneity of the particles led to overlapping internal distance distributions among particles with different radii. Correspondingly, the greater stability of the coformulated colloids allowed us to investigate preferential binding and release of protein–DNA, protein–peptide, and even protein– protein mixtures, speaking both to the mechanism of colloid association with biological macromolecules and potentially their use as purifying reagents.

RESULTS AND DISCUSSION

The Coformulated Colloids Are Monodisperse and Stable

To undertake these studies, we needed to overcome the polydispersity and transient stability of normal colloidal aggregates. Here, the dye coformulated colloids were crucial. Pure sorafenib or vemurafenib colloids, like most simple colloidal aggregates, have a wide range of radii. This is readily visualized by transmission electron microscopy (TEM) or by their broad and sometimes multipeaked DLS spectra. Instead, the coformulated colloids have particles with similar radii by TEM, and much narrower DLS spectra, as previously shown.[26] Consistent with these characteristics, we find by SAXS (Figure 1A,B) that the 25:1 coformulated sorafenib/Congo-Red (Sor/ CR) particles adopt a radius that varies slightly around 33 nm at concentrations ranging from 50 to 1000 μM sorafenib (2 to 40 μM Congo Red in the coformulated particles; Figure 1C). The observation that the particle radii do not change with concentration, by Guinier analysis, suggests that the colloidal particles were not themselves coassociating, supporting a direct analysis of their structure.

The Internal Structure of Colloidal Aggregates from SAXS

The greater size homogeneity of the coformulated colloids allowed us to investigate whether they were well-packed throughout the particle, resembling a fat droplet, or hollow, resembling a vesicle. Analysis of the SAXS spectra by the pair distance distribution function ($P(r)$), the distribution of the sum of interatomic distances in a particle, defines a form factor for the particle.[27] Both standard and coformulated colloidal aggregates appear spherical by TEM, with and without negative stain.[19,26,28] Spherical particles with a hollow core–shell structure have skewed interatomic distance distributions[26,29] relative to particles that are well-packed throughout, which have an essentially normal distribution of distances (Figure 2a). We observe by SAXS that the Sor/CR coformulated colloids conform much more closely to the normal distribution of the $P(r)$ expected of a well-packed, nonhollow particle (Figure 2b).

The Internal Structure of Colloidal Aggregates by MALS

Admittedly, even the coformulated colloids retain some polydispersity, and the SAXS spectra reflect the contributions of the $P(r)$ functions of all particle radii in the sample,[30] potentially confounding the analysis. So, we turned to dynamic and multiangle light scattering to further explore the question of colloid internal packing. The ratio of the radius of gyration (R_g) to the hydrodynamic radius (R_h) for a hard sphere is 0.77.[31–34] Consistent

with that expectation, our measurement of the R_g/R_h ratio by multiangle light scattering (MALS) for polysterene latex beads was 0.79 (Table 1). Conversely, we found that hollow polymeric micelles have an R_g/R_h ratio of 1.32. By MALS and SAXS the R_g/R_h ratio of Sor/CR colloids were 0.83 and 0.74, respectively (Table 1), supporting the conclusion that these colloid aggregates are well-packed structures, not hollow spheres.

Colloidal Aggregates Preferentially Sequester Protein vs DNA or Peptides

In addition to their relative monodispersity, coformulated colloids are much more stable than pure colloidal aggregates,[26] enabling them to bind protein, be isolated by centrifugation, and then be resuspended with protein still bound. This can be done multiple times, while even pelleting and resuspending once with active protein bound has been unachievable with pure colloidal aggregates. This new stability as a purifying reagent allowed us to investigate whether these particles would preferentially bind to protein or to DNA, or to whole folded protein versus peptides derived from that same protein. Such preferential binding has not previously been explored but seemed interesting both pragmatically, as a potential way to separate macromolecules from cellular and proteomic mixtures, and as a way to investigate driving forces in macromolecule–protein association. For instance, if macromolecule–colloid binding is driven by polar interactions, which after all drive dye-stacking, or by interactions involving the peptide bond, or if the macromolecules are buried in the interior of the colloids, one might expect peptides, especially more hydrophobic stretches, to preferentially bind to the colloids. Conversely, if binding is driven by association of the colloid with a large continuous surface, then one might expect proteins to bind better than peptides. Of course, a mixture of forces could be involved and the null hypothesis–and our expectation–was that the particle would bind both protein and peptides about equally. To our surprise, this was not the case.

To investigate the simpler question, whether the coformulated colloids would preferentially bind DNA or protein, we compared the binding of the globular domain of the ribosomal protein L2 (L2gd) labeled with fluorescein (5-MF-L2gd) to the binding of double-stranded DNA (dsDNA) also labeled with fluorescein (FAM-dsDNA). As Sor/CR concentration is increased, 5-MF-L2gd shows saturable fluorescence quenching, providing a sensitive readout for binding (Figure 3A, black curve). Conversely, the lack of fluorescence quenching on FAM-dsDNA indicates that the colloids do not bind to DNA or fluorescein itself (Figure 3A, blue curve). Correspondingly, when either FAM-dsDNA or indeed single-stranded DNA labeled with fluorescein (FAM-ssDNA) were exposed to 50 μM of the Sor/Cr colloids, no increase in fluorescence polarization was observed, in contrast to 5-MF-L2gd, which showed a large increase in polarization, consistent with the latter's sequestration on the colloids (Figure 3B). Consistent with these observations, when the colloids are mixed with a 1 Kb DNA ladder (lane 1, Figure 3C), spun down, and resuspended, no DNA is detected *via* gel electrophoresis in the detergent-disrupted colloidal pellet (lane 2, Figure 3C), rather all the DNA remains in the supernatant (lane 3, Figure 3C). Conversely, proteins are readily pelleted out of solution by the colloids, and they can be resuspended and released multiple times.[26] Indeed, when directly compared in competition with one another, the presence of even 20 μg/mL DNA had no effect on the amount of AmpC that was bound, spun-down, resuspended, and then detergent-released from the colloids. These observations

suggest that colloidal aggregates preferentially bind protein over either single-stranded or double-stranded DNA.

We then turned to the preferential binding of peptide or protein by the colloids. We compared a mixture of AmpC β-lactamase and eight synthetic peptides representing an AmpC protease digest,[25] mimicking a proteomic mixture between a protein and its component peptides. These eight peptides ranged in size from 8 to 20 amino acids (see Materials and Methods). We measured the ability of Sor/CR coformulated colloids to inhibit enzyme activity in the presence of peptides. If the colloidal aggregates bind peptide preferentially to an enzyme, or even about the same as an enzyme, we would expect the peptide mixture to reduce colloidal inhibition of the enzyme, as the peptides are present in great molar excess. Conversely, if the colloids bound enzyme much more strongly than peptides, we would expect the presence of the peptides to have little effect on the inhibition of the enzyme.

The Sor/CR colloids inhibited AmpC activity in the presence of peptides almost as well as they inhibited in the absence of peptides. Even a 1600-fold molar excess of the eight-peptide mixture, i.e., 200-fold excess in *each* of the eight peptides (AmpC present at 2 nM, peptides present at 400 nM each; 3.2 μM total peptide), had only a modest effect on colloidal inhibition of the enzyme (Figure 4A). Nor did the same peptide mixture much affect the ability of colloids to inhibit trypsin (Figure 4A). This was true not only of the Sor/CR coformulated colloids but also of standard monoformulated sorafenib and fulvestrant colloids (Table 2). The inability of the peptides to outcompete enzyme binding to the colloids contrasts with that of other unrelated proteins to do so. For instance, at 0.1 mg mL^{-1}, bovine serum albumin (1.6 μM), trypsin (4 μM), and egg white lysozyme (7 μM) almost entirely disrupt colloidal inhibition of AmpC by colloidal aggregates.[35] Indeed, whereas 3.2 μM peptide had only a modest effect on colloidal inhibition of β-lactamase, even 30 nM trypsin was sufficient to block β-lactamase inhibition by the colloids (Table 2). This presumably reflects the presaturation of colloid binding sites by trypsin, something the peptides could not do even at 100-fold higher concentration.

To ensure inhibition reflected direct enzyme-colloid binding, we centrifuged the Sor/CR colloids after exposure to either AmpC or to Trypsin and separated the precipitated colloids from the supernatant. The colloids were resuspended in fresh buffer, disrupted by detergent, and their residual activity measured. Whether the enzyme alone had been exposed to colloids, or as part of the peptide mixture, the activity measured after colloid disruption was only modestly affected (Figure 4B). This suggests that the colloids had directly bound close to the same amount of enzyme in the presence or absence of the peptides in 1600-fold molar excess, consistent with highly preferential binding of the proteins over the peptides.

A concern with these inhibition experiments was whether the colloids were fully saturated with enzyme. To address this, we turned to direct binding experiments where we could show full saturation of the colloids by protein. We first established the binding capacity of Sor/CR colloids to 5-MF-L2gd (SI Figure 1): 100 nM 5-MF-L2gd is fully quenched by 20 μM of Sor/CR (this is the concentration of monomeric sorafenib that goes into the Sor/CR colloids, the concentration of the colloid itself is subnanomolar[2]). We interpret this as the point of

colloid saturation by protein–beyond this concentration, no further protein is adsorbed by the colloids. To 20 μM of Sor/CR, we added increasing amounts of AmpC or of the AmpC peptides in the presence of 100 nM 5-MF-L2gd (all proteins and peptides added simultaneously). As the concentration of AmpC was raised, the amount of 5-MF-L2gd bound diminished linearly, as evidenced by the rising fluorescence (Figure 4C). Conversely, the mixture of peptides had no effect, even though in molar terms they were about 25-fold more concentrated than AmpC. To confirm this result, we also explored direct binding of the colloids to a 7-amino acid (HTFPAVL) fluorescein-labeled peptide. Unlike the 5-MF-L2gd protein, where the addition of 50 μM Sor/Cr colloids greatly increased the polarization signal from the labeled protein, no significant rise in peptide fluorescent polarizationwas observed, again suggesting no substantial sequestration of the peptide by the colloids (Figure 4D). This further supports the preferential binding of colloidal aggregates to folded proteins over peptides.

Investigators have long wondered if colloidal aggregates bind different proteins with different affinities. The heterogeneity and large size of colloidal particles has made this difficult to explore, and the simplest hypothesis has been that there is little or no protein specificity for colloids, other than that explained by the different protein concentrations used in different assays (given the stoichiometric inhibition by colloids, differences in protein concentration lead to different apparent IC_{50} values). With the homogeneity and small size of the coformulated colloids, we could tackle this question. We investigated the ability of four proteins–unlabeled L2gd, malate dehydrogenase, human serum albumin (HSA), and AmpC β-lactamase–to compete with the binding of 5-MF-L2gd to the Sor/CR colloids, again using fluorescent quenching as a readout. To our surprise, a 90-fold difference in apparent affinity was observed. The apparent EC_{50} for the L2gd protein itself was 0.024 mg mL^{-1}; for malate dehydrogenase, was 0.43 mg mL^{-1}; for HSA, was 0.95 mg mL^{-1}; and for AmpC, was projected to be 2.2 mg mL^{-1}. Expressing these concentrations in molar units changes the differences only modestly, with the range between L2gd and AmpC only falling to 40-fold.

Though colloidal aggregates of organic small molecules have been intensely studied,[2,4,5,25,26,36–50] their transient stability and heterogeneity have impeded our understanding of their structure and mechanism. The striking improvement in the size homogeneity and stability of coformulated colloidal aggregates enables investigation of properties that have long eluded the field. Four key observations emerge from these studies. Structurally, SAXS, MALS, and DLS analyses agree that the colloids are well-packed and not hollow. Mechanistically, the colloidal aggregates much prefer proteins over DNA or over peptides, even when those peptides are components of the proteins to which they are compared. Up to 1600-fold molar excess of peptide was insufficient to measurably disrupt the colloid's ability to bind and inhibit protein. This may suggest that colloids preferentially recognize the large surface features that proteins can better provide. Unexpectedly, we find a 90-fold difference in protein binding preference for the coformulated colloids, something that was previously difficult to observe but consistent with even the earliest observations in the field.[1] Finally, the preferential recognition of proteins over DNA or peptides lets one imagine actually optimizing colloidal aggregates for a useful purpose,[51,52] here to separate proteins from cellular or proteomic mixtures.

The conclusion that colloidal aggregates are essentially solid throughout is illuminating structurally and mechanistically. Even though colloids transit through a critical aggregation concentration (CAC),[2] a phase-like transition akin to a CMC, their filled core structure differs from that of vesicles and micelles. This has implications for their thermodynamics of formation and for our understanding of their binding stoichiometry. Once we assume that colloidal aggregates are solid throughout, the number of monomer molecules that they contain can be estimated based on their size, and from that the concentration of colloid may be estimated for any amount of monomer added above the CAC. The well-packed nature of the colloids also supports the idea that they act *via* an adsorptive surface phenomenon, something also suggested by stoichiometric considerations.[2]

The preferential binding of protein over peptide mixtures by colloids may further support a surface-based interaction with protein and casts light on the driving interactions. Cutting AmpC into component peptides from a protease digest, representing about 40% of the overall protein, makes its backbone amides more available and exposes runs of hydrophobic side chains that would ordinarily be buried. Even 400 nM of a peptide like VAFIPEKLEG, with its run of hydrophobic residues, was insufficient to block colloid sequestration of β-lactamase, whereas just 30 nM of trypsin was able to do so. Colloidal aggregates lead to limited protein unfolding, and it was at least conceivable that this was owed to preferential binding of the main chain amides. The lack of peptide binding argues against this. More surprisingly, even runs of hydrophobic residues seem insufficient to confer binding sufficient to keep with the intact protein. This supports the surface nature of colloid-protein recognition, which is where proteins would have an advantage over peptides, if only through avidity, and suggests that exposed hydrophobicity, in itself, is insufficient to explain protein sequestration. Mean-while, the strong preference for protein over dsDNA suggests that highly anionic species are not preferred, presumably because of desolvation penalties on bringing them to the colloid surface. Nor did even ssDNA, which largely eliminates costs for helix melting and exposes the DNA bases, bind strongly, consistent with a charge and a desolvation role in limiting colloidal association.

Astonishingly, we observed a two-log difference in apparent binding affinity for different proteins to the coformulated colloids. Whereas differences in apparent IC_{50} values for proteins had long been observed, the null hypothesis was that much of this could be explained by the different concentrations of the proteins in the assays, or different assay conditions. With the ability to measure binding directly, something enabled by the homogeneity and relatively small size–and hence low scattering–of the coformulated colloids, direct binding competition can now be undertaken. The strong binding of the L2gd protein may be partly explained by its relatively low folded stability in solution, while the better binding of HSA relative to AmpC may be partly explained by its relatively large hydrophobic surface. Naturally these explanations are for now very tentative, and a full investigation of the differential protein binding observed here, and its generality to other colloidal species, must await its own focused study.

Pragmatically, the increased stability of the coformulated colloids allows them to be treated as reagents that can be loaded with enzyme, centrifuged out of a mixture, and resuspended to release active enzyme. This cannot be done with classical colloidal aggregates. The ability to

preferentially and tightly sequester protein over both dsDNA and ssDNA, and over peptides, allows one to imagine their use in cellular or proteomic mixtures, acting to separate protein.

Certain caveats merit airing. Most importantly, the conclusions drawn based on the coformulated colloids used here cannot with certainty be extended to classic colloidal aggregates, as coformulation changes their properties. Still, coformulated and "pure" colloids do share many properties– they undergo a critical aggregation concentration, appear to be spherical,[26] and sequester and inhibit proteins. The same peptide mixture that does not substantially reduce the enzyme inhibition of a Sor/CR coformulation also does not reduce the enzyme inhibition by pure sorafenib or by pure fulvestrant colloids, supporting the similarity of the two classes of aggregates. Mechanistically, whereas the results of this study support a surface–surface interaction between the colloids and protein, we have not explicitly demonstrated that. Pragmatically, while the coformulated colloids can separate protein from DNA and protein from concentrated mixtures of peptides, and can chaperone protein through multiple handling steps (spin-down, resuspension, disruption-and-release), their loading capacity is substantially less than that of a simple pure colloidal aggregate at the same concentration. This will limit their usefulness until this can be better optimized.

These cautions should not obscure the major conclusions of this study–colloidal aggregates appear to be well-packed without an appreciable hollow core. They preferentially bind protein over DNA or peptides, likely through a surface interaction, and indeed, for the first time, can be shown to differentially bind different proteins. Whereas it may be greater polarity that distinguishes DNA from protein, hydrophobicity alone seems insufficient for recognition, a large surface interaction appears necessary for tight binding. The ability to sequester protein preferentially to DNA and peptides suggests that coformulated colloidal aggregates may be optimized for use in cellular or proteomic separation.

MATERIALS AND METHODS

Materials

Congo Red (Cat No. C6227), polystyrene latex beads with a mean radius of 100 nm (Cat NO. LB1), and Triton X-100 (Cat No. X100) were purchased from Sigma-Aldrich. Sorafenib (Cat No. HY-10201) was purchased from MedChem Express. AmpC β-lactamase was purified from *Escherichia coli* to apparent homogeneity, as described.[53] Trypsin (Cat No T0303) and Suc-Ala-Ala-Pro-Arg-pNA (Cat No. L1720) were purchased from Sigma-Aldrich and BACHEM, respectively. Eight synthetic peptides, the products of an AmpC protease digest,[25] were purchased from Genscript: IVHRTIT-PLIE, YADIAKKQPVTQQTL, YTAGGLPLQVPDEVKSSSDL, QNWQPAWAPGTQRL, KTLQQGIQ, LDWPVNPDSIINGS-DNAKIA, VAFIPEKLEG, and LANKNYPNPARVDAA. Polymeric micelles were composed on a graft copolymer, poly(D,L-lactide-*co*-2-methyl-2-carboxy-trimethylenecarbonate)-*g*-poly(ethylene glycol) (P(LA-*co*-TMCC)-*g*-PEG), that has an average of three PEG chains (each 10 kDa in length) per hydrophobic backbone.[48] The AmpC substrate CENTA was purchased from EMD Millipore (Cat No 219475). Except for AmpC, all materials were used as supplied by the manufacturer without further purification. The globular domain of bacterial ribosomal protein L2 (60–202 fragment, L2gd) was expressed from BL21(DE3) *E. coli* and purified as

an inclusion body. His-tagged L2gd was refolded while bound on Ni-NTA sepharose by washing with 20 mM Tris at pH 7.5, 50 mM KCl, and 5mM β-MeOH and eluted with the same buffer with 400 mM imidazole. Fluorescein labeling with 5-maleimide-fluorescein (5-MF) was done through a KCK peptide appended to the N-terminus of L2gd. Fluorescein-labeled dsDNA was prepared as described.[54] The seven-amino-acid peptide (HTFPAVL) is labeled at the N-terminus with fluorescein. This sequence was derived from a C_H1 domain of the IgG1 antibody.

Enzyme Assays

AmpC and trypsin activity assays were performed in 50 mM potassium phosphate (KPi, pH 7) buffer using CENTA and Suc-Ala-Ala-Pro-Arg-pNA as substrates, respectively, in a final reaction volume of 1 mL. A HP8453a spectrophotometer in kinetic mode using UV–Vis Chemstation software (Agilent Technologies) was used to monitor the rates of both reactions at 405 nm. First order reaction rates were calculated by linear regression using Chemstation. The colloid sedimentation and resuspension experiment was performed as described.[26]

Small Angle X-ray Scattering

SAXS data were collected on the Bio-SAXS beamline BL4-2 at Stanford Synchrotron Radiation Lightsource (SSRL) using a Rayonix MX225-HE CCD detector (Rayonix, Evanston, IL) with a sample-to-detector distance of 3.5 m and a beam energy of 8 keV (wavelength, λ = 1.550 Å). The momentum transfer (scattering vector) q was defined as $q = 4\pi \sin(\theta)/\lambda$, where 2θ is the scattering angle. All data were collected up to a maximum q of 0.028 $Å^{-1}$ (3.5 m sample-to-detector distance). The program GNOM was used to generate the pairwise distribution functions $P(r)$upto $q \sim 0.06$ $Å^{-1}$. The R_g of each sample was determined using Guinier's law, which included plotting ln $I(q)$ vs q^2 and calculating the slope of the line of best fit through data points 2– 6. All reported R_g values are within the limits of $qR_g < 1.3$. McSAS is Monte Carlo based analysis software performed on all SAXS profiles to obtain theoretical distribution of particles that will result in the scattering profile.[56,57]

Dynamic Light Scattering and Multiangle Light Scattering

Colloid and polystyrene bead hydrodynamic radii were measured using a DynaPro Plate Reader II (Wyatt Technology) with a 60 mW laser operating at 830 nm and detector angle of 158°; the width of the laser had been increased by the manufacturer to optimize detection of colloidal aggregates. All measurements were performed in a 384-well format (40 μL sample/well) at 25 °C. Regularization analysis was used to determine the R_h. Multiangle laser light scattering (MALS) measurements of colloid and polystyrene beads were made using a DAWN HELEOS II MALS detector (Wyatt Technology) at 4 °Cby directly injecting the samples into the flow cell. The detector employed a laser source at 658 nm and 18 photodetectors at angles between 22.5° and 147.0°. Output from all detectors were imported into ASTRA 6 (Wyatt Technology) for analysis. R_g's of the samples were determined by Zimm plots where linear regression was used to analyze the angular dependence of light scattering by multiple detectors. Extrapolation of the line of best fit to 0 angle (γ intercept) corresponds to the R_g.[58]

Direct Binding Assays for Colloidal Aggregates

Binding of protein, peptide, and DNA to Sor/CR colloids was determined *via* fluorescence quenching of 5-MF-L2gd, measured using a SpectraMax M5Microplate Reader, with wavelengths of excitation and emission set to 485 and 538 nm, respectively, and a 530 nm cutoff filter. The 40 μL/well samples were analyzed in 384-well plates, at RT. 5-MF-L2gd and FAM-dsDNA were incubated at 100 nM in 50 mM KPi buffer, at pH 7, with Sor/CR ranging in concentration from 0 to 60 μM.

To monitor fluorescence recovery as a measure of competitive binding, 100 nM of 5-MF-L2gd was mixed with increasing concentrations of competing protein or peptide, up to 1.25 mg mL^{-1}, in the presence of 20 μM Sor/CR.

Fluorescence polarization was used as the most direct measure of protein, peptide, and DNA binding to Sor/CR colloidal aggregates. Polarization of 75 nM 5-MF-L2gd and 100 nM FAM-peptide, FAM-ssDNA, and FAM-dsDNA was measured as a function of time in the absence and then presence of 50 μM Sor/CR using a Fluoromax-4 Spectrofluorometer (Jobin Yvon Technology). Excitation and emission of the fluorophore was set to 485 nm (5 nm slit) and 538 nm (5 nm slit), respectively. The 40 μL samples were analyzed in a Quartz cuvette, at RT, in 50 mM KPi, at pH 7.

Colloid Centrifugation and Gel Electrophoresis

The 50 μM Sor/CR was formulated in 50 mM KPi, at pH 7, incubated with 20 μg/ mL of 1 kb DNA ladder for 5 min at RT and pelleted by centrifugation at 16 000*g* for 1 h. The colloidal pellet was resuspended in KPi and 0.01% Triton X-100 to disrupt aggregates and release any bound DNA. Agarose gel electrophoresis was performed on the colloidal resuspension and supernatant.

Supplementary Material

Refer to Web version on PubMed Central for supplementary material.

Acknowledgments

Supported by U.S. National Institutes of Health grant GM071630 (to B.K.S. and M.S.S.) and by the Howard Hughes Medical Institute (to D.A.A.). We thank T. Matsui for his help collecting the SAXS data at SSRL BL4-2 and A. Lyon for helping collect the MALS data, M. O'Meara and J. Pottel for reading this manuscript, S. Isaac and G. Narlikar for providing labeled ssDNA and dsDNA, and E. Karagöz and P. Walter for providing labeled peptide, both for the binding assay.

References

1. McGovern SL, Caselli E, Grigorieff N, Shoichet BK. A common mechanism underlying promiscuous inhibitors from virtual and high-throughput screening. J Med Chem. 2002; 45:1712–1722. [PubMed: 11931626]
2. Coan KE, Shoichet BK. Stoichiometry and physical chemistry of promiscuous aggregate-based inhibitors. J Am Chem Soc. 2008; 130:9606–9612. [PubMed: 18588298]
3. Wolan DW, Zorn JA, Gray DC, Wells JA. Small-molecule activators of a proenzyme. Science. 2009; 326:853–858. [PubMed: 19892984]

4. McGovern SL, Helfand B, Feng B, Shoichet BK. A Specific Mechanism for Non-Specific Inhibition. J Med Chem. 2003; 46:4265–4272. [PubMed: 13678405]
5. Ryan AJ, Gray NM, Lowe PN, Chung C. Effect of Detergent on "Promiscuous" Inhibitors. J Med Chem. 2003; 46:3448–3451. [PubMed: 12877581]
6. Feng BY, Simeonov A, Jadhav A, Babaoglu K, Inglese J, Shoichet BK, Austin CP. A high-throughput screen for aggregation-based inhibition in a large compound library. J Med Chem. 2007; 50:2385–2390. [PubMed: 17447748]
7. Babaoglu K, Simeonov A, Irwin JJ, Nelson ME, Feng B, Thomas CJ, Cancian L, Costi MP, Maltby DA, Jadhav A, Inglese J, Austin CP, Shoichet BK. Comprehensive mechanistic analysis of hits from high-throughput and docking screens against beta-lactamase. J Med Chem. 2008; 51:2502–2511. [PubMed: 18333608]
8. Jadhav A, Ferreira RS, Klumpp C, Mott BT, Austin CP, Inglese J, Thomas CJ, Maloney DJ, Shoichet BK, Simeonov A. Quantitative analyses of aggregation, autofluorescence, and reactivity artifacts in a screen for inhibitors of a thiol protease. J Med Chem. 2010; 53:37–51. [PubMed: 19908840]
9. Ferreira RS, Simeonov A, Jadhav A, Eidam O, Mott BT, Keiser MJ, McKerrow JH, Maloney DJ, Irwin JJ, Shoichet BK. Complementarity between a docking and a high-throughput screen in discovering new cruzain inhibitors. J Med Chem. 2010; 53:4891–4905. [PubMed: 20540517]
10. Klumpp M. Non-stoichiometric inhibition in integrated lead finding – a literature review. Expert Opin Drug Discovery. 2016; 11:149–162.
11. Harpel, MR. Handbook of Drug Screening. 2nd. Seethala, R., Zhang, L., editors. CRC Press; Boca Raton, FL: 2016. p. 269-297.Ch. 10
12. Tritsch D, Zingle C, Rohmer M, Grosdemange-Billiard C. Flavonoids: true or promiscuous inhibitors of enzyme? The case of deoxyxylulose phosphate reductoisomerase. Bioorg Chem. 2015; 59:140–144. [PubMed: 25800132]
13. Zingle C, Tritsch D, Grosdemange-Billiard C, Rohmer M. Catechol-rhodanine derivatives: Specific and promiscuous inhibitors of Escherichia coli deoxyxylulose phosphate reductoisomerase (DXR). Bioorg Med Chem. 2014; 22:3713–3719. [PubMed: 24890653]
14. Baell JB, Holloway GA. New substructure filters for removal of pan assay interference compounds (PAINS) from screening libraries and for their exclusion in bioassays. J Med Chem. 2010; 53:2719–2740. [PubMed: 20131845]
15. Baell JB. Feeling Nature's PAINS: Natural Products, Natural Product Drugs, and Pan Assay Interference Compounds (PAINS). J Nat Prod. 2016; 79:616–628. [PubMed: 26900761]
16. Erlanson DA. Learning from PAINful lessons. J Med Chem. 2015; 58:2088–2090. [PubMed: 25710486]
17. McGovern SL, Shoichet BK. Kinase inhibitors: not just for kinases anymore. J Med Chem. 2003; 46:1478–1483. [PubMed: 12672248]
18. Seidler J, McGovern SL, Doman TN, Shoichet BK. Identification and prediction of promiscuous aggregating inhibitors among known drugs. J Med Chem. 2003; 46:4477–4486. [PubMed: 14521410]
19. Feng BY, Shelat A, Doman TN, Guy RK, Shoichet BK. High-throughput assays for promiscuous inhibitors. Nat Chem Biol. 2005; 1:146–148. [PubMed: 16408018]
20. Duan D, Doak AK, Nedyalkova L, Shoichet BK. Colloidal aggregation and the in vitro activity of traditional Chinese medicines. ACS Chem Biol. 2015; 10:978–988. [PubMed: 25606714]
21. Ilevbare G, Taylor L. Liquid–liquid phase separation in highly supersaturated aqueous solutions of poorly water-soluble drugs: Implications for solubility enhancing formulations. Cryst Growth Des. 2013; 13:1497–1509.
22. Ilevbare GA, Liu H, Pereira J, Edgar KJ, Taylor LS. Influence of additives on the properties of nanodroplets formed in highly supersaturated aqueous solutions of ritonavir. Mol Pharmaceutics. 2013; 10:3392–3403.
23. Raina SA, Alonzo DE, Zhang GG, Gao Y, Taylor LS. Using Environment-Sensitive Fluorescent Probes to Characterize Liquid-Liquid Phase Separation in Supersaturated Solutions of Poorly Water Soluble Compounds. Pharm Res. 2015; 32:3660–3673. [PubMed: 26123681]

24. Shoichet BK. Interpreting steep dose-response curves in early inhibitor discovery. J Med Chem. 2006; 49:7274–7277. [PubMed: 17149857]
25. Coan KE, Maltby DA, Burlingame AL, Shoichet BK. Promiscuous aggregate-based inhibitors promote enzyme unfolding. J Med Chem. 2009; 52:2067–2075. [PubMed: 19281222]
26. McLaughlin CK, Duan D, Ganesh AN, Torosyan H, Shoichet BK, Shoichet MS. Stable Colloidal Drug Aggregates Catch and Release Active Enzymes. ACS Chem Biol. 2016; 11:992–1000. [PubMed: 26741163]
27. Pedersen JS. Analysis of small-angle scattering data from colloids and polymer solutions: modeling and least-squares fitting. Adv Colloid Interface Sci. 1997; 70:171–210.
28. Doman TN, McGovern SL, Witherbee BJ, Kasten TP, Kurumbail R, Stallings WC, Connolly DT, Shoichet BK. Molecular Docking and High-Throughput Screening for Novel Inhibitors of Protein Tyrosine Phosphatase-1B. J Med Chem. 2002; 45:2213–2221. [PubMed: 12014959]
29. Mittelbach R, Glatter O. Direct structure analysis of small-angle scattering data from polydisperse colloidal particles. J Appl Crystallogr. 1998; 31:600–608.
30. Kikhney AG, Svergun DI. A practical guide to small angle X-ray scattering (SAXS) of flexible and intrinsically disordered proteins. FEBS Lett. 2015; 589:2570–2577. [PubMed: 26320411]
31. Bloomfield VA. Static and dynamic light scattering from aggregating particles. Biopolymers. 2000; 54:168–172. [PubMed: 10861377]
32. Burchard W, Schmidt M, Stockmayer WH. Information on Polydispersity and Branching from Combined Quasi-Elastic and Integrated Scattering. Macromolecules. 1980; 13:1265–1272.
33. Burchard W. Polymer Characterization — Quasi-Elastic and Elastic Light-Scattering. Makromol Chem, Macromol Symp. 1988; 18:1–35.
34. Hirzinger B, Helmstedt M, Stejskal J. Light scattering studies on core-shell systems: determination of size parameters of sterically stabilized poly(methylmethacrylate) dispersions. Polymer. 2000; 41:2883–2891.
35. Coan KE, Shoichet BK. Stability and equilibria of promiscuous aggregates in high protein milieus. Mol BioSyst. 2007; 3:208–213. [PubMed: 17308667]
36. Frenkel YV, Clark AD Jr, Das K, Wang YH, Lewi PJ, Janssen PA, Arnold E. Concentration and pH dependent aggregation of hydrophobic drug molecules and relevance to oral bioavailability. J Med Chem. 2005; 48:1974–1983. [PubMed: 15771441]
37. Liu HY, Wang Z, Regni C, Zou X, Tipton PA. Detailed kinetic studies of an aggregating inhibitor; inhibition of phosphomannomutase/phosphoglucomutase by disperse blue 56. Biochemistry. 2004; 43:8662–8669. [PubMed: 15236574]
38. Reddie KG, Roberts DR, Dore TM. Inhibition of kinesin motor proteins by adociasulfate-2. J Med Chem. 2006; 49:4857–4860. [PubMed: 16884297]
39. Giannetti AM, Koch BD, Browner MF. Surface Plasmon Resonance Based Assay for the Detection and Characterization of Promiscuous Inhibitors. J Med Chem. 2008; 51:574–580. [PubMed: 18181566]
40. Chan LL, Lidstone EA, Finch KE, Heeres JT, Hergenrother PJ, Cunningham BT. A method for identifying small molecule aggregators using photonic crystal biosensor microplates. Conf Proc IEEE Eng Med Biol Soc. 2009:788–791. [PubMed: 19964243]
41. Thorne N, Inglese J, Auld DS. Illuminating insights into firefly luciferase and other bioluminescent reporters used in chemical biology. Chem Biol. 2010; 17:646–657. [PubMed: 20609414]
42. Miller JR, Thanabal V, Melnick MM, Lall M, Donovan C, Sarver RW, Lee DY, Ohren J, Emerson D. The use of biochemical and biophysical tools for triage of high-throughput screening hits — A case study with Escherichia coli phosphopantetheine adenylyltransferase. Chem Biol Drug Des. 2010; 75:444–454. [PubMed: 20486930]
43. Combs AP. Recent advances in the discovery of competitive protein tyrosine phosphatase 1B inhibitors for the treatment of diabetes, obesity, and cancer. J Med Chem. 2010; 53:2333–2344. [PubMed: 20000419]
44. Jiang J, Ganesh T, Du Y, Thepchatri P, Rojas A, Lewis I, Kurtkaya S, Li L, Qui M, Serrano G, Shaw R, Sun A, Dingledine R. Neuroprotection by selective allosteric potentiators of the EP2 prostaglandin receptor. Proc Natl Acad Sci U S A. 2010; 107:2307–2312. [PubMed: 20080612]

45. Coan KE, Ottl J, Klumpp M. Non-stoichiometric inhibition in biochemical high-throughput screening. Expert Opin Drug Discovery. 2011; 6:405–417.
46. Meireles LMC, Mustata G. Discovery of modulators of protein-protein interactions: current approaches and limitations. Curr Top Med Chem. 2011; 11:248–257. [PubMed: 21320056]
47. LaPlante SR, Aubry N, Bolger G, Bonneau P, Carson R, Coulombe R, Sturino C, Beaulieu PL. Monitoring drug self-aggregation and potential for promiscuity in off-target in vitro pharmacology screens by a practical NMR strategy. J Med Chem. 2013; 56:7073–7083. [PubMed: 23919803]
48. Logie J, Owen SC, McLaughlin CK, Shoichet MS. PEG-Graft Density Controls Polymeric Nanoparticle Micelle Stability. Chem Mater. 2014; 26:2847–2855.
49. Julien O, Kampmann M, Bassik MC, Zorn JA, Venditto VJ, Shimbo K, Agard NJ, Shimada K, Rheingold AL, Stockwell BR, Weissman JS, Wells JA. Unraveling the mechanism of cell death induced by chemical fibrils. Nat Chem Biol. 2014; 10:969–976. [PubMed: 25262416]
50. Bisson J, McAlpine JB, Friesen JB, Chen SN, Graham J, Pauli GF. Can Invalid Bioactives Undermine Natural Product-Based Drug Discovery? J Med Chem. 2015; 59:1671. [PubMed: 26505758]
51. Shi J, Du X, Huang Y, Zhou J, Yuan D, Wu D, Zhang Y, Haburcak R, Epstein IR, Xu B. Ligand-receptor interaction catalyzes the aggregation of small molecules to induce cell necroptosis. J Am Chem Soc. 2015; 137:26–29. [PubMed: 25522243]
52. Kuang Y, Long MJ, Zhou J, Shi J, Gao Y, Xu C, Hedstrom L, Xu B. Prion-like nanofibrils of small molecules (PriSM) selectively inhibit cancer cells by impeding cytoskeleton dynamics. J Biol Chem. 2014; 289:29208–29218. [PubMed: 25157102]
53. Powers RA, Blazquez J, Weston GS, Morosini MI, Baquero F, Shoichet BK. The complexed structure and antimicrobial activity of a non-beta-lactam inhibitor of AmpC betalactamase. Protein Sci. 1999; 8:2330–2337. [PubMed: 10595535]
54. Isaac RS, Jiang F, Doudna JA, Lim WA, Narlikar GJ, Almeida R. Nucleosome breathing and remodeling constrain CRISPR-Cas9 function. eLife. 2016; 5doi: 10.7554/eLife.13450
55. Svergun DI. Determination of the Regularization Parameter in Indirect-Transform Methods Using Perceptual Criteria. J Appl Crystallogr. 1992; 25:495–503.
56. Bressler I, Pauw BR, Thunemann AF. software for the retrieval of model parameter distributions from scattering patterns. J Appl Crystallogr. 2015; 48:962–969. [PubMed: 26089769]
57. Pauw BR, Pedersen JS, Tardif S, Takata M, Iversen BB. Improvements and considerations for size distribution retrieval from small-angle scattering data by Monte Carlo methods. J Appl Crystallogr. 2013; 46:365–371. [PubMed: 23596341]
58. Wyatt PJ. Light-Scattering and the Absolute Characterization of Macromolecules. Anal Chim Acta. 1993; 272:1–40.

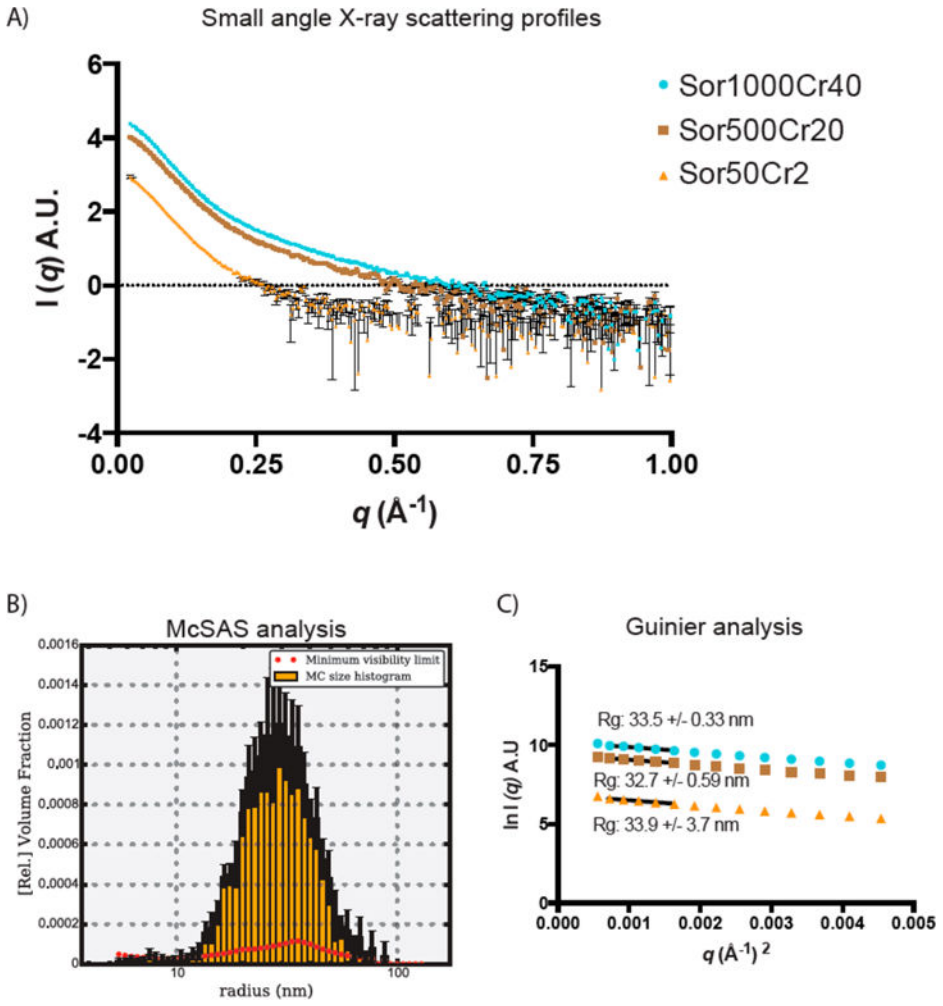

Figure 1.

Small-angle X-ray scattering from the coformulated colloids supporting a more homogeneous population of particles. (A) SAXS scattering profiles of Sor/CR colloids at three different concentrations within q range of 0.028–1 $Å^{-1}$. SAXS scattering profiles of Sor/CR (25:1, 1000 μM sorafenib), Sor/CR (25:1, 500 μM sorafenib), and Sor/CR (25:1, 50 μM sorafenib) are in cyan, brown, and orange, respectively. (B) McSAS anaylsis of SAXS scattering profile of Sor/CR (25:1, 1000 μM sorafenib) colloids using only the first 170 data points. (C) Guinier analysis using only data points 2–6 of all three scattering profiles to obtain radius of gyration. All spectra taken in 50 mM KPi, pH 7.0.

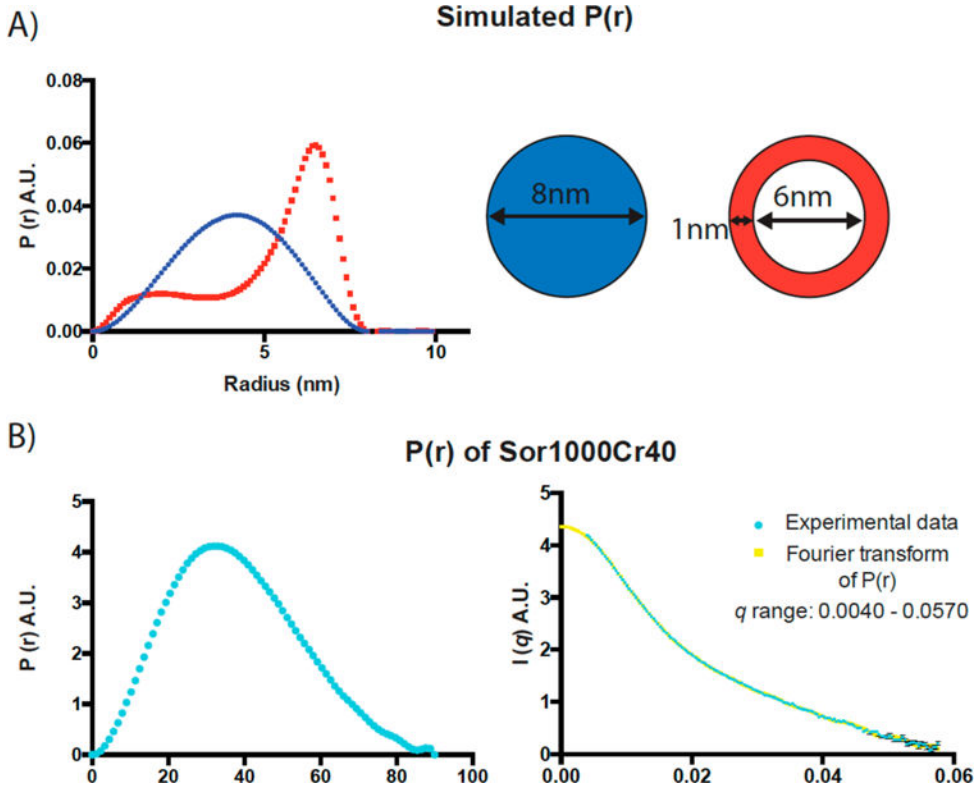

Figure 2.

The SAXS spectra, supporting a filled core structure for the colloidal particles. (A) Simulated *P*(*r*) functions for two particles of the same diameter but different cores-shell structures. (B) Left panel is *P*(*r*) function obtained from SAXS scattering profile of Sor/CR (25:1; 1000 μM sorafenib) colloids in the *q* range of 0.0040–0.0570 $Å^{-1}$. Right panel shows a good fit between Fourier transformed *P*(*r*) in the left panel and the raw SAXS scattering data, indicating that the *P*(*r*) is an accurate representation of the scattering profile.

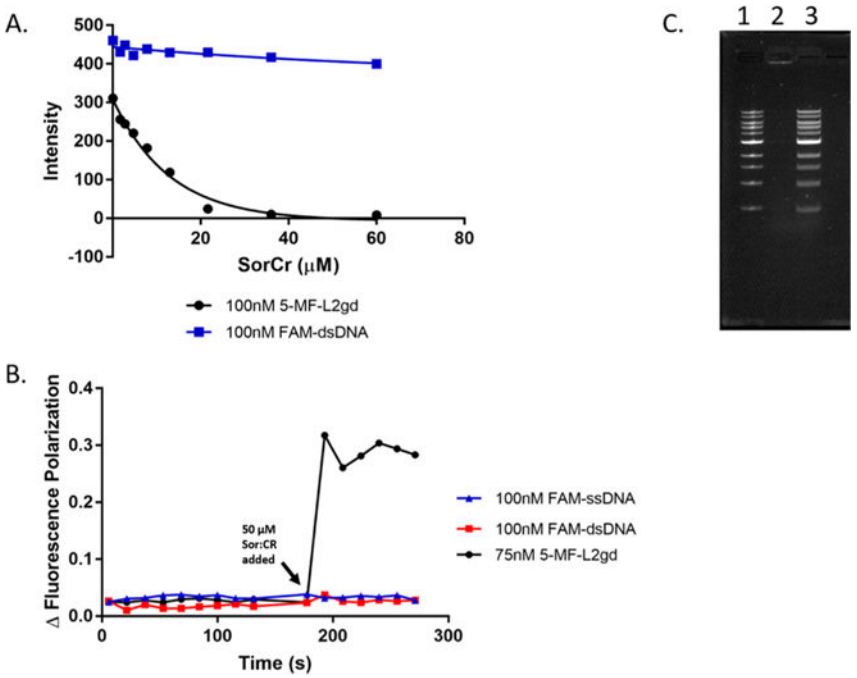

Figure 3.

Colloids preferentially bind protein versus DNA (A) The fluorescence intensity of fluorescein-labeled L2gd protein (5-MF-L2gd, black curve), but not fluorescein labeled dsDNA (FAM-dsDNA, blue curve), is quenched in the presence of increasing amounts of Sor/CR colloidal aggregates. (B) Whereas the addition of 50 μM Sor/CR colloids significantly increases the polarization of 5-MF-L2gd protein, the colloids had little measurable effect on the polarization of dsDNA or ssDNA also labeled with fluorescein. (C) Incubation with 1 Kb DNA ladder (lane 1, precolloids) and subsequent spin-down and resuspension of the colloidal pellet yields no DNA (lane 2). Instead, DNA is detected in the supernatant (lane 3).

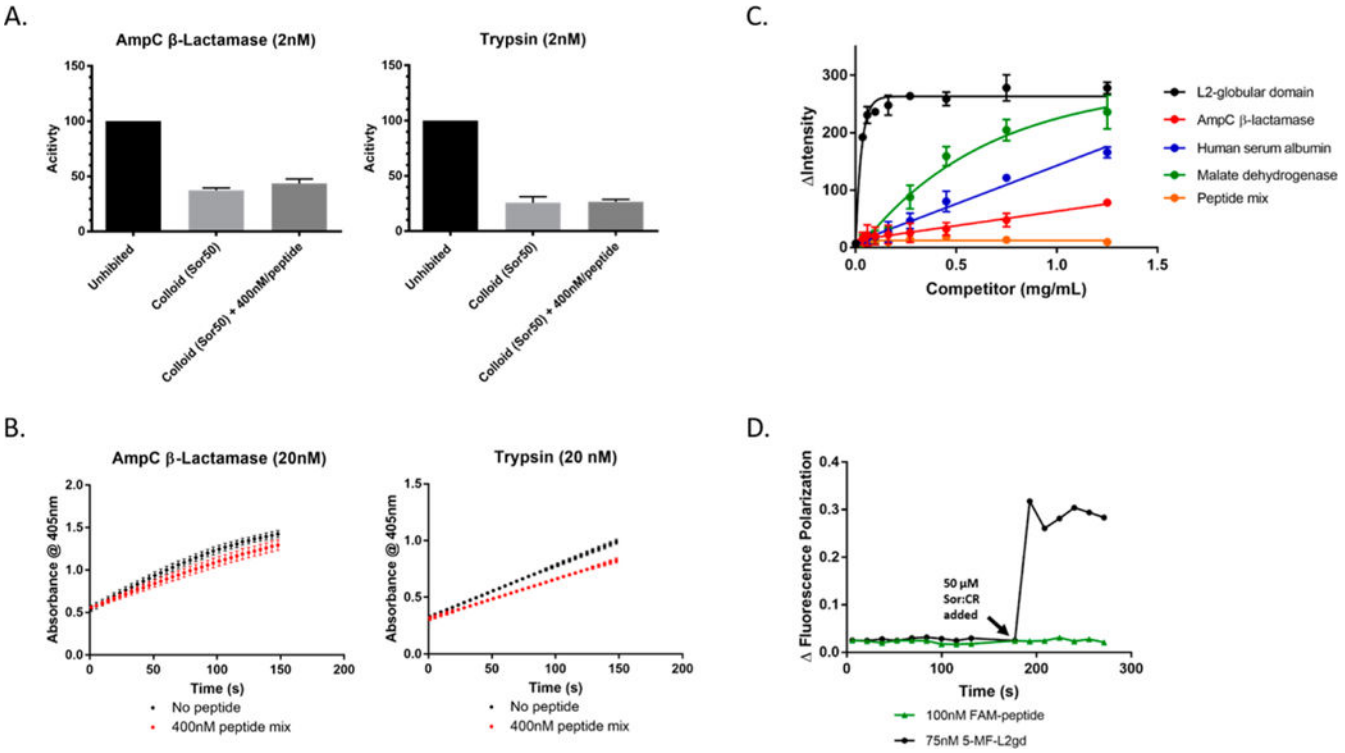

Figure 4.

Colloids preferentially protein versus peptides. (A) The amounts of inhibited activity of 2 nM of AmpC β-lactamase or 2 nM trypsin by Sor/CR (25:1, 50 μM sorafenib) colloids in the presence and absence of 400 nM peptide mixture do not exhibit major differences. (B) Spin-down experiment where 20 nM of AmpC β-lactamase or trypsin was incubated with Sor/CR (25:1, 500 μM sorafenib) for 5 min in the presence and absence of 3.2 μM of the eight peptide mixture (400 nM in each of the eight peptides). The solution is centrifuged, and the resulting pellet is resuspended in buffer. Colloid disruption by 0.01% Triton X-100 releases the enzymes back into solution, and only slight differences are observed between the activity of samples with and without the peptide mixture. (C) The competitive displacement of labeled 5-MF-L2gd on the colloid by other proteins increases its fluorescence. Shown is competition with unlabeled L2gd itself, human serum albumin, malate dehydrogenase, and AmpC β-lactamase. The large range in apparent IC_{50} values supports differential binding by different proteins. Meanwhile, the eight peptide mixture has little measurable ability to compete with protein for colloid binding. (D) Consistent with this observation, the addition of 50 μM Sor/CR colloids substantially increases the polarization of 5-MF-L2gd protein but had little measurable effect on the polarization of the labeled HTFPAVL peptide, suggesting that the latter does not bind to the colloid.

Table 1

R_g to R_h Ratio of Sor/CR Colloids Is Consistent with Hard Spheres

	R_g avg ± (nm)	R_h avg ± (nm)	R_g/R_h
polystyrene latex beads (100 nm diameter)	44.4 ± 1.4	56.6 ± 2.7	0.79
SorCR (25:1, 50 μM sorafenib) colloids	38.2 ± 6.7 (MALS) 33.9 ± 3.7 (SAXS)	45.5 ± 1.0	0.83 (MALS)/ 0.74 (SAXS)
polymeric micelles	49.6 ± 8.6	37.7 ± 0.58	1.32

Table 2

Enzyme Inhibition by Coformulated and Pure Colloids with and without Peptide

colloid	competitor	inhibition of 2 nM AmpC (%)	inhibition of 2 nM trypsin (%)
50 μM Sor/ Cr	none	56.6 ± 4.5	80.1 ± 1.7
	3.2 μM peptide mix	50.1 ± 2.1	76.4 ± 1.1
	30 nM trypsin	15.8 ± 2.2	
5 μM Sorafenib	none	90.8 ± 1.1	42.4 ± 6.1
	3.2 μM peptide mix	77.5 ± 2.7	37.3 ± 6.2
	30 nM trypsin	15 ± 5.9	
5 μM Fulvestrant	none	57.1 ± 3.7	33.9 ± 7.8
	3.2 μM peptide mix	45.6 ± 6.8	33.6 ± 8.0
	30 nM trypsin	12.5 ± 2.4	